TANG HUMANITAS MEDICINE

Original Article

Ethanolic extract of Condurango (*Marsdenia condurango*) used in traditional systems of medicine including homeopathy against cancer can induce DNA damage and apoptosis in non small lung cancer cells, A549 and H522, *in vitro*

Sourav Sikdar[1], Avinaba Mukherjee[1], Naoual Boujedaini[2], Anisur Rahman Khuda-Bukhsh[1,*]

[1]*Cytogenetics and Molecular Biology Laboratory, Department of Zoology, University of Kalyani, Kalyani-741235, India;* [2]*Boiron Laboratory, Lyon, France*

ABSTRACT

In traditional systems of medicine including homeopathy, the Condurango extract (Con) is often used to cure stomach cancer mainly, without having any scientific validation of its anti-cancer ability. Con has therefore been tested against non-small-cell lung cancer cells (NSCLC) A549 and NCI-H522 (H522) known to contain the KRAS mutation, making them resistant to most chemotherapeutic agents. As cancer cells generally defy cytotoxicity developed by chemopreventive agents and escape cell death, any drug showing the capability of preferentially killing cancer cells through apoptosis is worth consideration for judicious application. A549 and H522 cells were exposed to 0.35 µg/µl and 0.25 µg/µl of Con, respectively, for 48 h and analysed based on various protocols associated with apoptosis and DNA damage, such as MTT assay to determine cell viability, LDH assay, DNA fragmentation assay, comet assay, and microscopical examinations of DNA binding fluorescence stains like DAPI, Hoechst 33258 and acridine orange/ethidium bromide to determine the extent of DNA damage made in drug-treated and untreated cells and the results compared. Changes in mitochondrial membrane potential and the generation of reactive oxygen species were also documented through standard techniques. Con killed almost 50% of the cancer cells but spared normal cells significantly. Fluorescence studies revealed increased DNA nick formation and depolarized membrane potentials after drug treatment in both cell types. Caspase-3 expression levels confirmed the apoptosis-inducing potential of Con in both the NSCLC lines. Thus, overall results suggest considerable anticancer potential of Con against NSCLC *in vitro*, validating its use against lung cancer by practitioners of traditional medicine including homeopathy.

Keywords anticancer potential, Condurango extract**,** A549 and NCI-H522 non small-cell lung cancer cells, apoptosis, DNA damage, reactive oxygen species, mitochondrial membrane potential

INTRODUCTION

Cancer is one of the dreaded diseases and affects more than ten million people annually (Misra et al., 2010), of which lung cancer is the most commonly diagnosed cancer with 1.4 million new cases reported each year (http://www.who.int/mediacentre/factsheets/fs297/en/index.html). It is currently the leading cause of cancer related deaths in the United States (Whitehead et al., 2003). Different types of carcinogens present in tobacco smoke are the main suspects to cause lung cancer (Kometani et al., 2009; Yang et al., 2000). Clinically, lung cancer is of two types, namely, small cell lung cancer (SCLC) and non small cell lung cancer (NSCLC). NSCLC accounts for >80% of all lung cancers and is responsible for more deaths from cancer than any other tumor types (Jemal et al., 2005). This type of cancer hardly responds to chemotherapy, primarily because of its KRAS mutation that often makes it resistant to chemotherapy (Guo et al., 2008). Traditionally surgery, radiation therapy, and chemotherapy are the ultimates to treat patients with NSCLC. But these treatments are usually accompanied by many side-effects. Many cancer patients are now treated with complementary and alternative medicine (CAM) for its less toxic side-effects. Different preparations of herbal extracts including homeopathy are some of the most popular CAM modalities for cancer patients in seven out of 14 European countries today (Rostock et al., 2011). However, many of these herbal extracts used as homeopathic mother tinctures have not been scientifically validated. Therefore, scientific approaches to test the efficacy of such plant extracts for their anti-cancer potentials, *in vitro*, are of utmost importance for the initial screening. The drugs that show such potentials should further be tested in animal models *in vivo*, so that the benefits from their therapeutic use can be justified in human cases. Furthermore, many of these natural products are known to have less adverse side-effects, and therefore, a further study of their possible cytotoxicity in normal and cancer cell lines may become more meaningful and significant.

Traditional herbal medicines are rich sources of new drugs. There is increasing interest in investigating different species of plants used as traditional medicines to identify effective ingredients using the most modern chemical and molecular methods (Wang et al., 2004). Literature suggests that the methanolic extract of *Marsdenia condurango* bark exhibits differentiation-inducing activity in M1 cells (Umehara et al., 1994). Condurango has long been used against a variety of

[*]Correspondence: Anisur Rahman Khuda-Bukhsh
E-mail: prof_arkb@yahoo.co.in; khudabukhsh_48@rediffmail.com
Received December 5, 2012; **Accepted** February 21, 2013; **Published** February 28, 2013
doi: http://dx.doi.org/10.5667/tang.2012.0044

digestive and stomach problems by local people as traditional and alternative medicine. Condurango was first introduced into the United States as a traditional medicine in 1871 for its ability to ameliorate stomach cancer and syphilis (Umehara et al., 1994). According to Banerji et al. (2008), Condurango is now being used to treat oesophageal cancer. However, the ethanolic extract of Condurango, which is occasionally used to treat patients showing symptoms of stomach cancer, had not been either validated scientifically in *in vitro* or *in vivo* systems earlier, or had not been tested in any lung cancer cell line, indicating their scope for use in a wider perspective on cancer (Banerji et al., 2008).

Apoptosis, or programmed cell death, is a common form of eukaryotic cell death. It is a physiological 'cell suicide' programme that helps to maintain homeostasis, in which cell death naturally occurs during tissue turnover (Samali et al., 1996; Staunton et al., 1998). Cells undergoing apoptosis usually show several cellular changes, including formation of plasma membrane blebs, reduction in cell volume, chromatin condensation, and DNA fragmentation. Apoptosis is regulated by various gene products including pro-(p53, Bcl_2, and Bax) and anti-(Bcl_2, Bcl_{XL}) apoptotic genes. The increased or decreased expressions of the above mentioned genes or proteins, respectively, trigger apoptosis (Staunton et al., 1998; White, 1996). Over-expression of the Bax results in the enhancement of reactive oxygen species (ROS) generation and the facilitation of cytochrome-c release (Jurgensmeier et al., 1998). Recently, Li et al., (1997) reported that the increase in the generation of ROS can also disrupt the mitochondrial membrane potential (Li et al., 1997).

As one of the hallmarks of cancer is the immortalization of cells that also do not have to depend on a supply of nutrients to proliferate, an important landmark of all anti-cancer drugs is their ability to induce apoptosis in these. Therefore, one major way through which the initial screening is done is by the assessment of the ability of the drug in inducing cell death in established cancer cell lines. Further, because of the ability of many anti-cancer drugs to induce apoptosis through pronounced DNA damage, any drug that can induce the fragmentation of DNA and increased caspase-3 expression virtually qualifies it to be a potentially anti-cancer drug.

Thus, in fine, in the present investigation, the hypotheses to be tested were: i) whether Condurango is able to induce apoptosis in the two NSCLC cancer cell lines, A549 and H522, ii) if it can induce apoptosis through extensive DNA damage and depolarization of mitochondrial membrane potential, and iii) if it has the ability to generate reactive oxygen species (ROS).

MATERIALS AND METHODS

Chemicals and reagents

Dulbecco's modified Eagle medium (DMEM), Roswell Park Memorial Institute-1640 (RPMI-1640), fetal bovine serum (FBS), 0.05% trypsin-EDTA, were purchased from Gibco BRL (Grand Island, NY, USA). The antibiotic antimicotic solution was purchased from Himedia, India. Cell culture plastic wares were obtained from Tarsons (USA). All organic solvents used were of 99% HPLC grade. Acridine orange (AO), 3-(4, 5-Dimethyl-thiazol-2-yl)-2, S-diphenyltetrazolium bromide (MTT), ethidium bromide (EB), Rhodamine 123, 4′,6-Diamidino-2-phenylindole dihydrochloride (DAPI), Hoechst 33258, dichloro-dihydrofluorescein diacetate (H_2DCFDA) and all other chemicals used were purchased from Sigma Chemical Co. (St. Louis, MO, USA).

Cell culture

A549 and NCI-H522 (H522) human lung carcinoma cell lines were procured from the National Centre for Cell Science (NCCS), Pune, India. A549 cells were cultured in DMEM and H522 cells were cultured in RPMI 1640, supplemented with 10% heat inactivated FBS and 1% antibiotic antimicotic solution maintained at 37℃ with 5% CO_2 in a humidified incubator. Cells of both types were harvested with a 0.05% trypsin-EDTA solution in phosphate buffer saline (PBS) and plated as the required cell numbers and allowed to adhere for 48 h before treatment.

Drug

We used homeopathic mother tincture, Condurango, procured from Boiron Laboratory, Lyon, France. They prepared the drug adopting the guidelines of European Pharmacopeia (http://www.pharmabooks.com.br/livros/images/livros/Index_7th_Edition_70.pdf) and supplied the drug in a 65% ethanolic extract, for which 65% ethanol was used as the "placebo".

Determination of cell viability

Cell viability was determined by MTT assay. A549 and H522 cells were dispensed in 96-well flat bottom microtiter plates at a density of 1×10^4 cells per well. After 48 h of incubation, they were treated with various concentrations of Con for 24 and 48 h incubation, to determine the concentration of Con at which the percentage of cell death was nearly 50%. Negative control cells received no drug i.e., untreated group (UT) and placebo (alcohol percentage at which the herbal extract is dissolved) treated group (PL) were also taken for this experiment. After treatment at 24 h and 48 h intervals, 10 µL of a MTT solution (1 mg/ml) was added to each well. The intracellular formazan crystals formed were solubilized with acidic isopropanol and the absorbance of the solution was measured at 595 nm (Mosmann, 1983) using an ELISA plate reader (Multiscan EX, Thermo Electron Corporation, USA). The relative percentages of viability were calculated.

Peripheral blood mononuclear cells (PBMC) analysis

Inbred healthy albino mice (*Mus musculus*), 3 to 4 months old, weighing between 20 gm and 30 gm, were reared under proper hygienic condition in polypropylene cages (temperature, 24 ± 2°C; humidity, 55 ± 5%, 12 h light/dark cycles) in the Animal House of the Department of Zoology, University of Kalyani; they were allowed free drinking water and basal diet *ad libitum*. Ethical clearance was obtained from the Institutional Ethical Committee, University of Kalyani (registration number-892/OC/05/CPCSEA) for the experimental set up. PBMC were isolated from the mice blood sample (99% homology with human) by the conventional ficol-gradient method (Biswas et al., 2011). The cells were plated in a 96-well plate with 5% RPMI media and incubated over night in a humidified CO_2 incubator (5% CO_2) at 37℃ under ambient oxygen levels. Then the cells were treated with Con at different concentrations and incubated for 24 h. The percentages of cell death were determined by conventional MTT assay and OD was taken at 595 nm by using an ELISA plate reader (Multiscan EX, Thermo Electron Corporation, USA) (Chakraborty et al., 2012).

Lactate dehydrogenase (LDH) activity-based cytotoxicity assay

LDH activity was assessed using a standardized kinetic determination kit (Enzopak, Recon, India). LDH activity was measured in both floating dead cells and viable adherent cells. The floating cells were collected from the culture medium by centrifugation (1000 g) at 4℃ for 5 min, and the LDH content

from the pellets was used as an index of apoptotic cell death (LDHa). The LDH released in the culture supernatant (LDHn) was used as an index of necrotic death, and the LDH present in the adherent viable cells was designated as intracellular LDH (LDHi) (Kim et al., 1997). The percentages of apoptotic and necrotic cell deaths were calculated as follows:

Observation of Morphological Changes

A549 and H522 cells were plated in six-well culture plates (1×10^3 cells per well) in DMEM and RPMI, respectively, supplemented with 10% FBS for 48 h. The cells were treated with Con at three different doses, IC_{50} value (D2), below IC_{50} value (sub-lethal dose, D1) and above IC_{50} value (D3) with untreated and placebo treated control groups. After 48 h of drug treatment, the cells were observed under an inverted phase contrast microscope at 40 magnification (Axiscope plus 2, Zeiss, Germany) and photographs were taken (Biswas et al., 2011).

DNA damage analysis by comet assay

The cells were trypsinized and washed with PBS after 48 h of drug treatment. The cell suspension was mixed with an equal amount of 1% low melting agarose kept at 37°C. 100 µl of the cell suspension was pipetted on to the slide precoated with normal melting agarose immediately after mixing. Then the cell suspension was covered with cover slips and immersed in a cold lysis buffer (2.5 M Nacl, 100 mM EDTA, 10 mM Tris, PH-10, with freshly added 1% Triton X-100 and 2% DMSO) followed by incubation at 4°C for at least 1h. The electrophoresis preceded a weak alkali (0.03 M NaOH, 1 mM EDTA, PH-12) at 1 V/cm and 30 mA for 15 min by a 20 min immersion of the slides in an electrophoresis buffer to promote chromatin unwinding. After electrophoresis, the slides were neutralized in a 0.05 M Tris buffer. After that, DNA was stained with ethidium bromide (5 mg/ml) for 10 min, washed with distilled water and examined under a fluorescence microscope at 40 magnification (Lyca, USA) (Biswas et al., 2011; Morley et al., 2006).

DNA fragmentation assay

Both groups of cells were treated with various concentrations of Con for 48 h after the growth at 70% confluence level. Following this treatment, the cells were washed twice with phosphate-buffered saline (PBS) left on ice for 15 min, and pelleted by centrifugation (1,000 g) at 4°C. Cell pellets were incubated with a DNA lysis buffer (10 mM Tris (pH 7.5), 400 mM NaCl, 1 mM EDTA and 1% Triton X-100) for 30 min on ice and then centrifuged (1500g) at 4°C. The supernatant was incubated overnight with RNase (0.2 mg/ml) and proteinase K (0.1 mg/ml) for 2 h at 37°C. DNA was extracted using the conventional phenol/chloroform method. Finally, the DNA was separated in a 2% agarose gel containing ethidium bromide and visualized under a UV transilluminator (Chakraborty et al., 2012).

Changes in nuclear morphology

To determine the chromatin condensation and DNA nick formation, cells under treatment were stained separately with DAPI and Hoechst 33258 stains (10 µg/ml). DAPI and Hoechst 33258 stains have the capacity to bind with the DNA nicks and fluoresce. After 48 h of drug treatment, the cells were stained and observed under a fluorescence microscope at 40 magnification (Axiscope plus 2, Zeiss, Germany). The representative photographs were taken for further quantitative analysis (Biswas et al., 2011).

Acridine orange/ethidium bromide (AO/EB) staining assay

For the further determination of DNA nick formation after drug exposure, AO/EB staining was done. After 48 h of drug treatment, cells were stained and observed under a fluorescence microscope at 40 magnification (Axiscope plus 2, Zeiss, Germany) against untreated controls. The representative photographs were taken for further quantitative analysis (Chen et al., 2007).

Study on ROS accumulation

H522 and A549 cells were treated with Con at three different doses for 24 h as ROS accumulation is the early event of apoptosis (Ling et al., 2003). Both groups of cells were incubated with 2′,7′-dichlorodihydrofluoresceindiacetate (H_2DCFDA) (5 mM) for 15 min. Then the potentials of D1, D2 and D3 to generate oxidative stress in terms of intracellular H_2O_2 generation were observed under a fluorescence microscope and photographs were taken at 40X magnification (Biswas et al., 2011).

Changes in mitochondrial membrane potential (Δψm)

The changes in mitochondrial membrane potential of the treated cells in contrast to untreated and only placebo treated cells were observed by a fluorescent probe, Rhodamine 123. As mitochondrial membrane potential is the early event of apoptosis generation and simultaneously occurs with ROS generation, the changes in the Δψm were observed at an early hour interval of drug treatment (24 h) (Bolduc et al., 2004). Briefly, 1 m/mol Rhodamine 123 was added to the cells (2×10^4) and was incubated for 15 min. Finally, the cells were observed under a fluorescence microscope at 40 magnification (Axioscope plus 2, Zeiss) and photographs were taken (Denning et al., 2002).

Western blot of caspase-3

As caspase-3 is one of the important markers of apoptosis and is known to activate at the last phase of apoptosis, we studied the changes of caspase-3 expression in both cell-types treated with different concentrations of Con against an untreated control at the 48 h interval. For Western blot analysis, equal amounts of protein of both cell types were loaded and samples were denatured in 15% SDS-PAGE for caspase-3 and GAPDH. The separated proteins were transferred to PVDF membranes and were probed with anti-caspase-3, and anti-GAPDH (1:1000) primary antibodies overnight at 4°C followed by 2 h incubation with HRP-conjugated secondary antibodies (1:500) and were developed by the DAB-H_2O_2 system. GAPDH was used as housekeeping gene control. Quantification of the proteins was done by densitometry, using image J software (Germany) (Su et al., 2006).

Statistical analysis

Data were analyzed and significance of the differences between the mean values was determined by one-way analysis of variance (ANOVA) with LSD post hoc tests, using SPSS 14 software (SPSS Inc, Chicago, IL, USA). Statistical significance was considered at $^*p < 0.05$ vs. untreated control group and $^{\#}p < 0.05$ vs. placebo treated group.

RESULTS

Effect of Con on cellular viability and LDH release

To check the cell viability of A549 and H522 after Con treatment, MTT assays were performed at 24 h and 48 h incubations with different doses, which in turn helps to determine the lethal dose at 50% level (IC_{50}) (fig. 1A-D). But in the case of 24 h drug treatment, the IC_{50} value was much

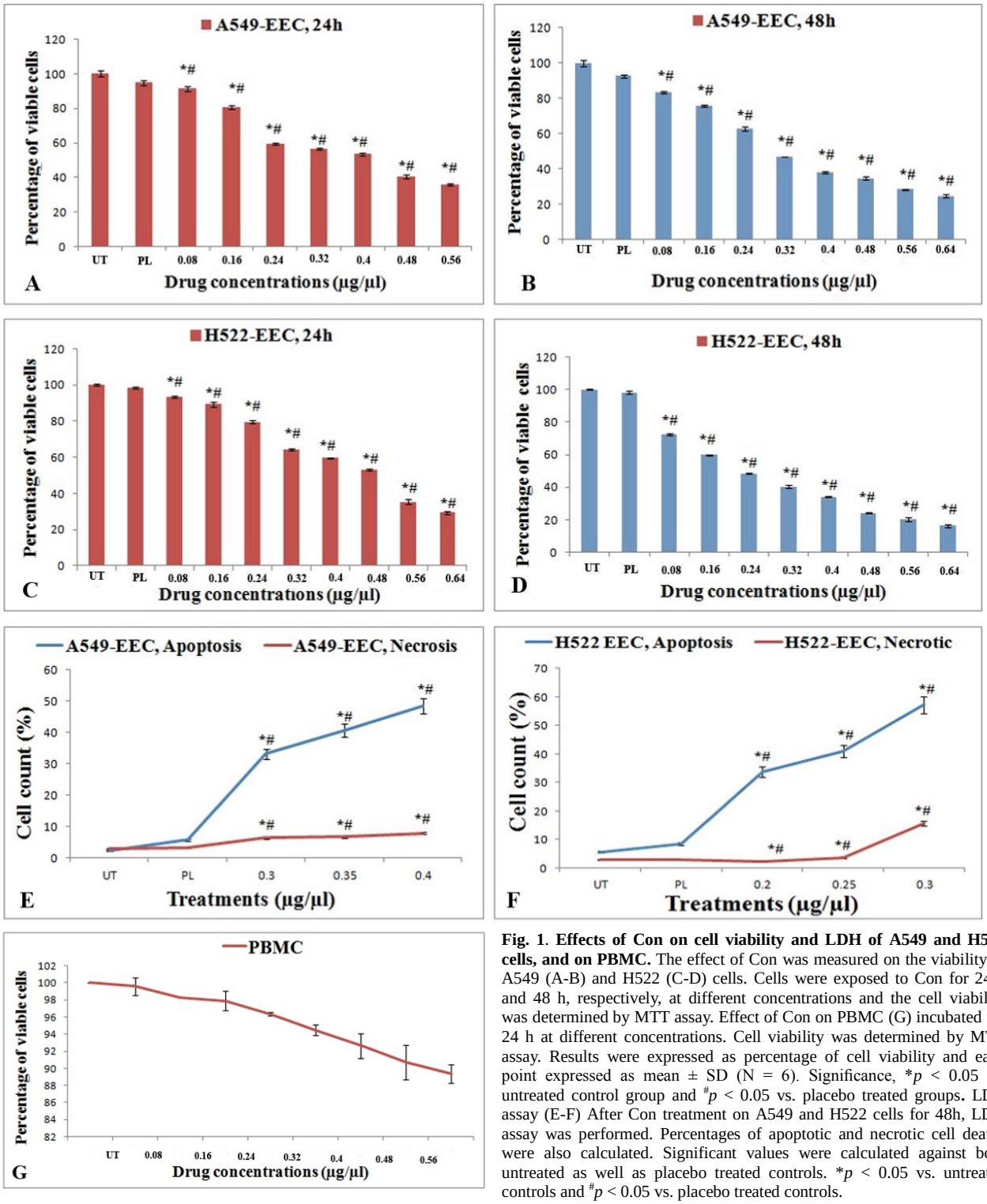

Fig. 1. **Effects of Con on cell viability and LDH of A549 and H522 cells, and on PBMC.** The effect of Con was measured on the viability of A549 (A-B) and H522 (C-D) cells. Cells were exposed to Con for 24 h and 48 h, respectively, at different concentrations and the cell viability was determined by MTT assay. Effect of Con on PBMC (G) incubated for 24 h at different concentrations. Cell viability was determined by MTT assay. Results were expressed as percentage of cell viability and each point expressed as mean ± SD (N = 6). Significance, *$p < 0.05$ vs. untreated control group and $^{\#}p < 0.05$ vs. placebo treated groups**.** LDH assay (E-F) After Con treatment on A549 and H522 cells for 48h, LDH assay was performed. Percentages of apoptotic and necrotic cell deaths were also calculated. Significant values were calculated against both untreated as well as placebo treated controls. *$p < 0.05$ vs. untreated controls and $^{\#}p < 0.05$ vs. placebo treated controls.

more to select the dose for further study. In the present study, the drug doses are represented at 48 h of incubation as D1, D2 and D3 for Con in the case of both H522 and A549 cell lines. The selected drug doses for further experiment were 0.20 µg/µl (D1), 0.25 µg/µl (D2-IC_{50}) and 0.30 µg/µl (D3) for H522 cell and 0.3 µg/µl (D1), 0.35 µg/µl (D2- IC_{50}) and 0.4 µg/µl (D3) in case of A549 cells. The cytotoxicities of D1, D2 and D3 were also checked for PBMC, which showed minimal effect (Fig. 1G). To further characterize D1, D2, and D3 treated A549 and H522 cell deaths, the ratios of LDH released from apoptotic and necrotic cells were compared (Fig. 1e and f). There was a significant ($p < 0.05$) increase in the ratio of apoptotic cells for D1, D2, and D3, but those of necrotic cells was still negligible in the presence of all the doses of D1, D2, and D3 in both types of cell lines. This assay indicates that the drug induced cell viability reduction is more apoptotic rather necrotic in nature.

Analysis of morphological changes

The morphological changes of A549 and H522 cells treated with D1, D2 and D3 were also observed with respect to

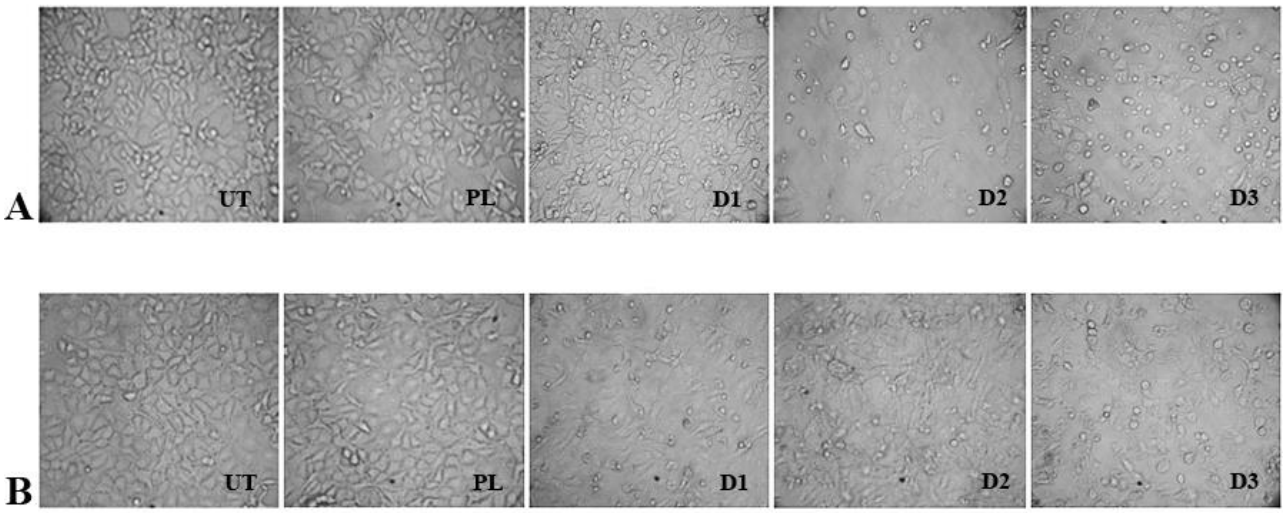

Fig. 2. Analysis of cellular morphology by phase-contrast microscopy at 48h of treatment. (A) represented the morphological differences of A549 cells and (B) represented the morphological differences of H522 cells. UT-untreated, PL- placebo treated control, D1- below IC50 value, D2- IC50 value and D3- above IC50 value.

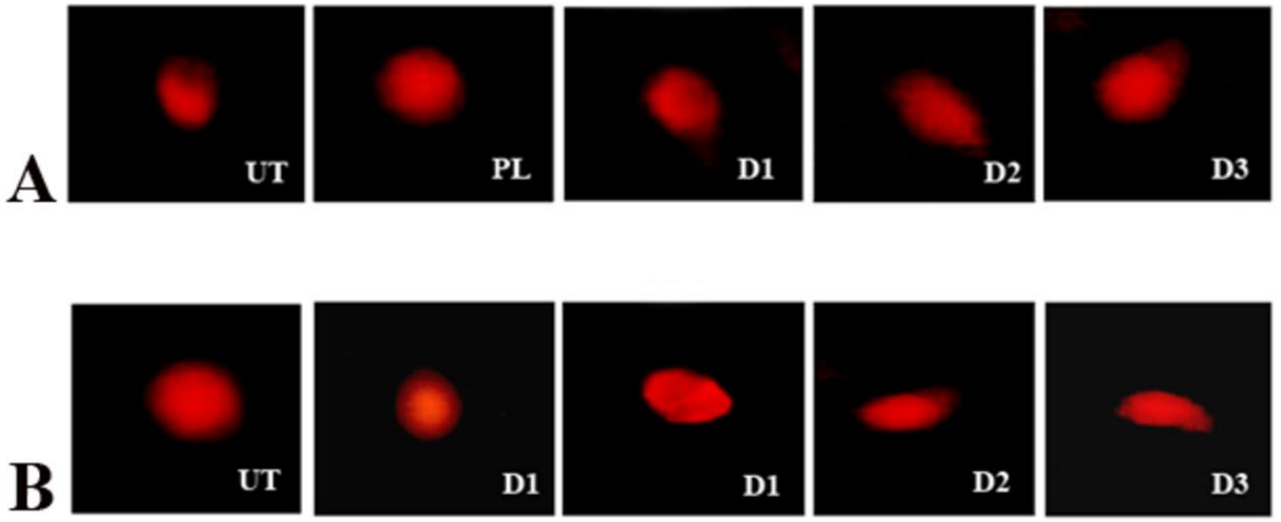

Fig. 3. Assessment of DNA damage by comet assay. (A) represented the comet tail formation with the increase of drug dose in H522 cells and (B) represented the comet tail formation with the increase of drug dose in A549 cells.

untreated cells and only placebo treated controls. Results revealed the morphological changes were typical of apoptosis (Fig. 2). Exposure to D1, D2 and D3 for 48 h caused the majority of A549 cells to shrink, become rounded up or elongated and detached from the culture dish with the increase of drug dose. But H522 cells became shrunken, deformed or rounded up after exposure to D1, D2 and D3.

DNA damage analysis by comet assay

It was observed that the nuclei were intact and roundish without any damaged DNA in the cases of untreated and placebo treated H522 and A549 cells after fluorescence microscopy. But in the Con treated cells, the comet tail lengths were observed and gradually increased with the increase of drug doses showing the signs of DNA damage which is the positive signal towards apoptosis (Fig. 3).

Analysis of DNA fragmentation assay

The DNA fragmentation was tested by agarose gel electrophoresis (Fig. 4) which indicates a significant increase in the inter-nucleosomal DNA fragmentation with the increase of drug doses in both H522 and A549 cells. This type of DNA ladder formation is one of the major events of apoptotis generation (Fig. 4).

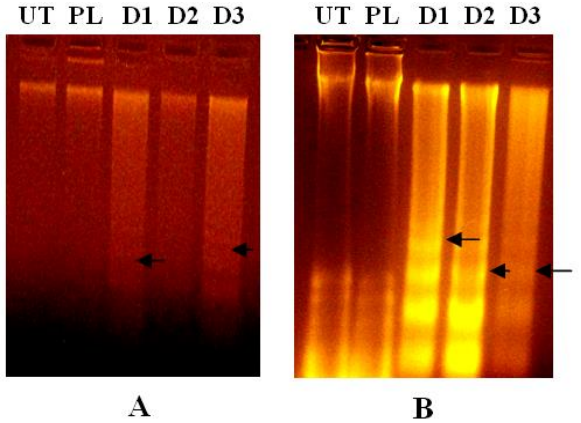

Fig. 4. DNA fragmentation assay. (A) denoted the increase of DNA fragmentation with Con treatment in H522 cells and (B) denoted the increase of DNA fragmentation with Con treatment in A549 cells at 48 h. The representative arrows indicated the fragmented DNA.

Nuclear morphology study by DAPI and Hoechst 33258 staining

Fluorescence microscopical study of DAPI and Hoechst 33258 staining revealed that the fluorescent intensities of DAPI and Hoechst 33258 were gradually increased with the increase of drug doses in both types of NSCLC lines. This observation clearly suggests the formation of DNA nick after Con treatment, which is indicative of the cells' journey towards apoptosis (Fig.

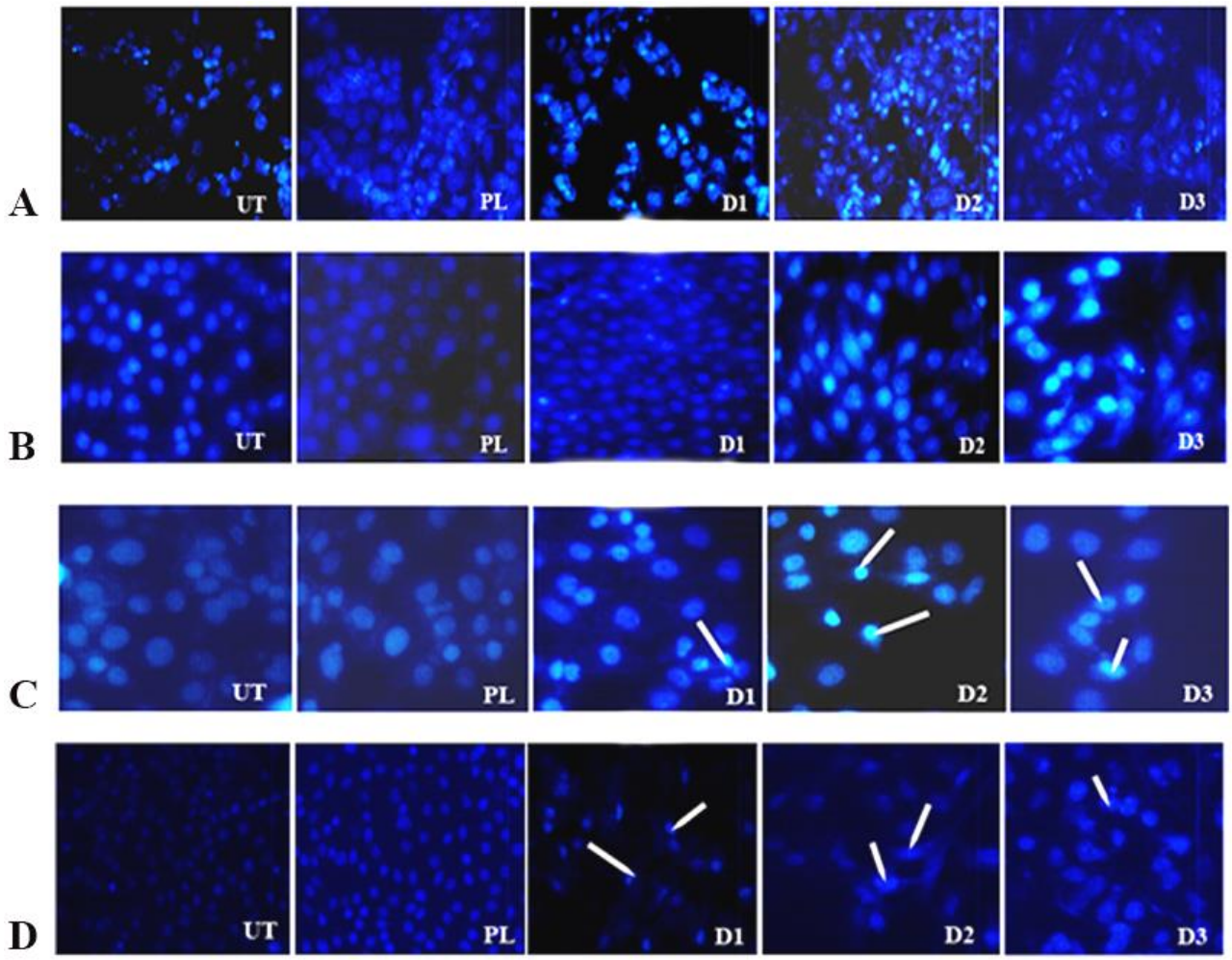

Fig. 5. Changes in nuclear morphology observed by DAPI and Hoechst 33258 staining. (A and B) represent the increase of DNA nick with the increase of drug dose in H522 and A549 cells respectively stained by DAPI; (C and D) represent the increase of DNA nick with the increase of drug dose in H522 and A549 cells respectively stained by Hoechst 33258. The representative arrows denotes the DNA nicks and nuclear deformities.

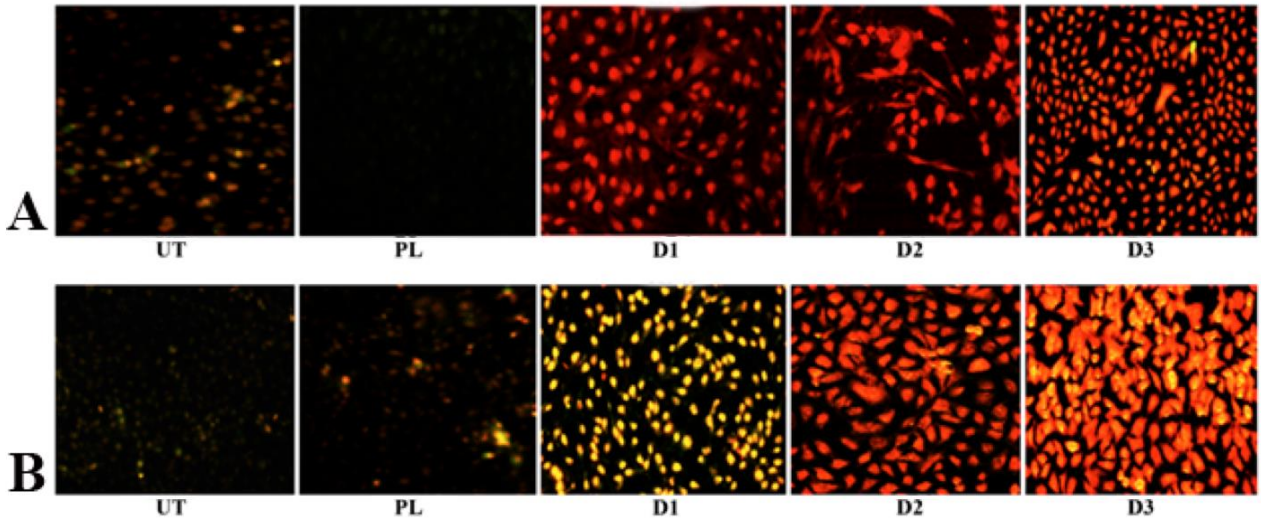

Fig. 6. AO-EB staining assay. Changes in the fluorescence pattern were observed from green (normal cellular DNA) to orange (nicked cellular DNA) along with increasing fluorescence intensity of ethidium bromide. The gradual increase of the florescence intensity in the drug treated cells in both H522 (A) and A549 (B) cells indicated the fragmentation of DNA and DNA nick generation.

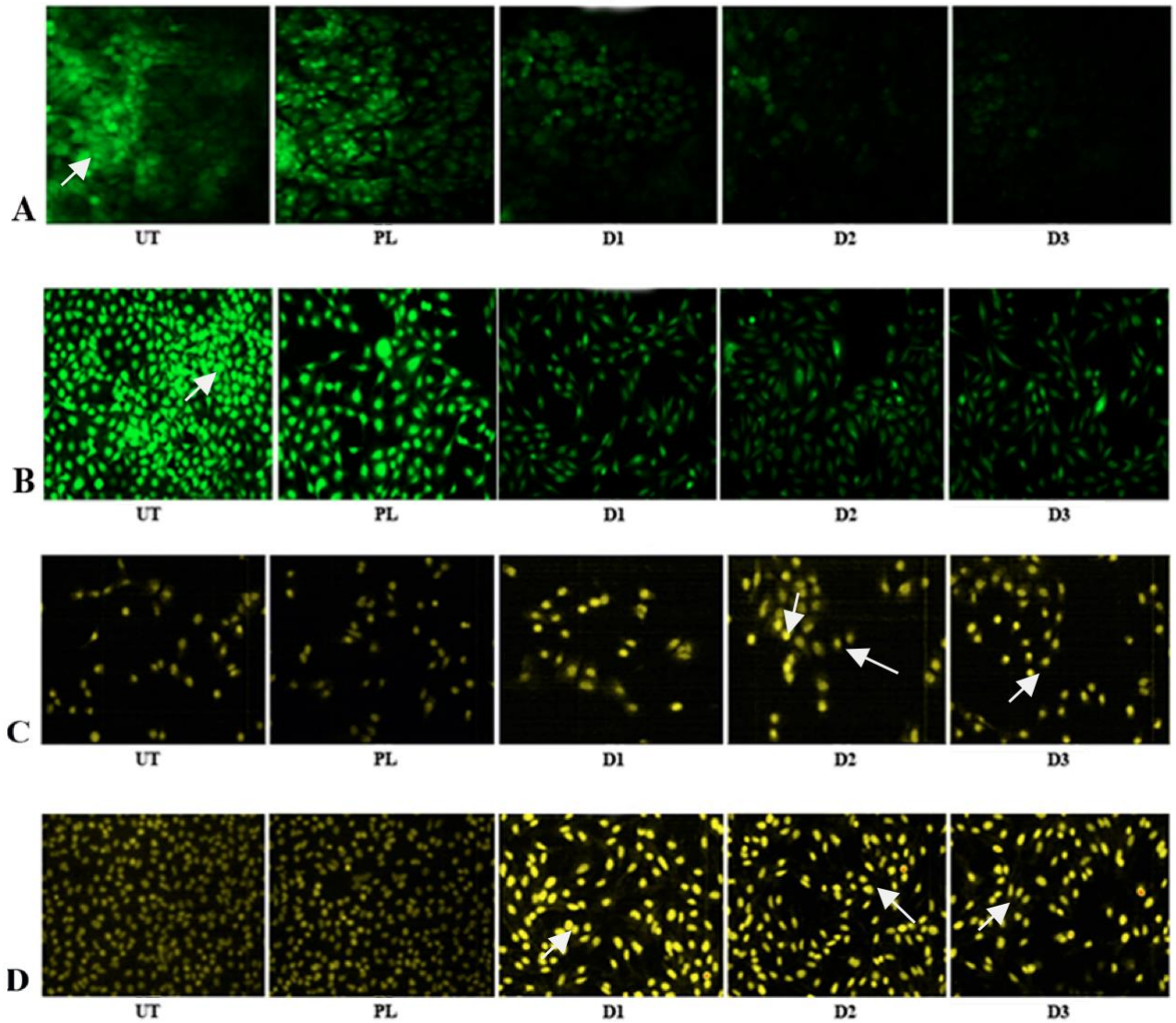

Fig. 7. Assessment of mitochondrial membrane depolarization (MMP) and ROS accumulation. H522 and A549 cells were treated with different concentrations of the drug along with untreated controls for 24h incubation. The cells were stained with Rhodamine 123 for MMP analysis and H_2DCFDA for the estimation of ROS. (A and B) represent the gradual decrease of MMP in H522 and A549 cells, respectively, with the increase of drug dose. (C and D) represented the gradual increase of ROS accumulation with the drug dose at 24h in H522 and A549 cells respectively.

5).

Analysis of AO/EB staining

Fig. 6 shows the changes in the fluorescence pattern from green (normal cellular DNA) to orange (nicked cellular DNA) along with increasing fluorescence intensity of ethidium bromide (red). The gradual increase of the florescence intensity in the drug treated cells in both A549 and H522 cells indicates the fragmentation of DNA and DNA nick generation. In the cases of untreated and only placebo treated cells, the fluorescence intensity was quite low due to the absence of damaged DNA. But in the case of D3, the cells completely took the red fluorescence, indicating thereby the complete fragmentation of DNA.

Analysis of ROS accumulation

The prevailing notion implicates intracellular ROS as signalling intermediates that are involved in signal transduction pathways of apoptosis. It was observed that there was no such generation of ROS in Con untreated and placebo treated cells. But the Con treated cells at three different doses showed intense staining and fluorescent property of H_2DCFDA as compared to the control, signifying the accumulation of ROS (Fig. 7). This positive signal supports the mitochondrial membrane depolarization, release of cytochrome-c and trigger apoptosis in a positive way.

Analysis of changes in mitochondrial membrane potential (Δψm)

The potential of D1, D2 and D3 to generate stress and the collapse of mitochondrial membrane potential before cell killing, and release of cytochrome-c from the mitochondria to the cytosol were measured using the fluorescent indicator Rhodamine 123 stain in both types of NSCLC lines at 24 h. The changes in MMP were observed with the increase of drug doses compared to untreated and placebo treated controls. Fluorescence microscopical study (Fig. 7) revealed that there were significant decreases in the green fluorescence intensity with the increase of drug doses as compared to the untreated and placebo treated control. This gradual decrease in the green fluorescence in drug treated samples indicates the mitochondrial membrane depolarization which is the early event of apoptosis.

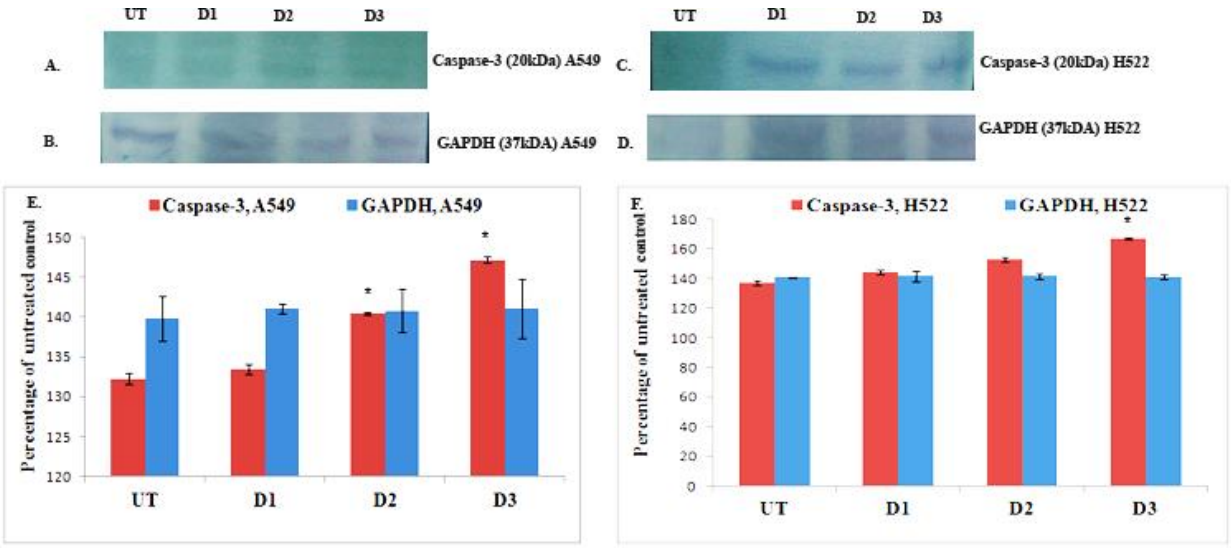

Fig. 8. Study on caspase-3 expression by Western blot. H522 and A549 cells were treated with different concentrations of Con maintaining untreated control for 48 h and the level of caspase-3 expression was determined by Western blot analysis. (A and C) represent the caspase-3 expression in different drug dose treated cells against untreated cells in both A549 and H522 cells, respectively, with GAPDH as house-keeping gene (B and D). The band intensities presented in the graph (E and F) showed significant an increase of caspase-3 expression after drug treatment in A549 and H522 cells, respectively. The results shown in the histograms are the average ± SD. Significance $*p < 0.05$ untreated (UT) vs different drug doses (D1, D2, D3)

Analysis of caspase-3 expression by Western blot

With the gradual increase of the Con doses, there was a concomitant increase in expressions of caspase-3 in both NSCLC cell types as compared to untreated control. This would indicate this drug induced apoptosis is possibly due to up-regulating caspase-3 expression (Fig. 8).

DISCUSSION

To our knowledge, this is the first study to evaluate the anti-cancer potentials of an ethanolic extract of Condurango on two NSCLC cell lines, *in vitro*. Although the drug is generally used in patients with symptoms of stomach cancer, its apoptotic effect on these two types of NSCLC cells observed in this study is significant, necessitating further scientific probe in other animal models with induced lung cancer, to examine if it could be equally effective against lung cancer *in vivo*.

In the present study we have investigated the cytotoxic effects of Con on H522 and A549 cell lines at 24 h and 48 h intervals. We have found the growth inhibitory effect of Con on H522 and A549 cells, as shown by the decrease in cell viability. In the case of 24 h drug treatment, the IC_{50} value (0.422 µg/µl for H522 and 0.469 µg/µl for A549) was much more than the 48 h IC_{50} (0.25 µg/µl for H522 and 0.35 µg/µl for A549) value to select the dose for further study. Thus, 48 h of drug exposure selecting three drug doses (D1, D2, and D3) which were relatively non-cytotoxic against normal PBMC was considered for further experimentation. An MTT assay suggests the decrease in the cell viability with the increase of drug treatment in respect to untreated and only placebo treated groups at 48 h of drug exposure. This result was supported by the LDH assay, where the apoptosis percentage was gradually increased in a drug dose-dependent manner. These results are the primary screening to establish the Con as an apoptosis-inducing agent against lung cancer *in vitro*. The morphological changes of both cell types gave support to the growth inhibiting properties of Con. The structural variations of drug treated cells against untreated controls seem to be indicative of its apoptosis pathway.

One of the major indications of apoptosis is the inter-nucleosomal DNA breakdown reported earlier (Yeh and Yen, 2005). DNA fragmentation assay and comet assay clearly suggest the induction of apoptosis in NSCLC after the gradual increase of Con treatment against untreated controls. DAPI and Hoechst stains have the affinity to bind with fragmented DNA during apoptosis. The fluorescence microscopical study shows the increased fluorescence intensity of DAPI and Hoechst with the increase of drug doses in both NSCLC lines; denoting thereby that this drug possibly acts through the induction of apoptosis for killing the cells. The drug targets the DNA of the cells, fragments it and gradually causes condensation of the nuclear mass, causing depolarization and change in the membrane potential and ultimately to an overall morphological change of the cell that leads finally towards apoptosis. In the present study, the AO-EB staining demonstrated the changes in fluorescence pattern from green to orange along with increased fluorescence intensity of ethidium bromide. This happens only when the DNA nick formation occurs and it occurs only during apoptosis. Generally, in the intrinsic (mitochondria-dependent) pathway of apoptosis, up-regulation and down-regulation of Bax and Bcl_2, respectively, occurs; this in turn triggers the cytochrome-c release which activates caspase-3 and caspase-9 and increases the intracellular free calcium. The increased expression of caspase-3 at the protein level would further confirm that the drug induced apoptosis via modulation of caspase-3 in both types of cell lines. This incident triggers the PARP cleavage which is the ultimate of the mitochondria dependent apoptotic pathway (Li et al., 1997). We conducted this study on mitochondrial membrane depolarization microscopically at the early time-point with the IC_{50} value. But the 24 h interval gave the best result of mitochondrial membrane depolarization. Then we performed the dose-dependent mitochondrial membrane potential study by fluorescence microscopy. This showed clearly that the mitochondrial membrane depolarization increases with the increase of drug dose in the two types of NSCLC cells as compared to the untreated controls. It also appears that the mitochondrial control mechanisms underlying apoptosis are involved in the disruption of mitochondrial membrane permeabilization, and the alteration in mitochondrial membrane transition pores, leading to the release of protein effectors

(Kroemer and Reed, 2000; Susin et al., 1998). The accumulation of ROS, which are the by-products of normal cellular oxidative processes, have been suggested as regulating the process involved in the initiation of apoptotic signaling. Tan and co-workers (Tan et al., 1998) showed that an increase in the generation of ROS induces cytochrome c release from mitochondria at early stages. Our experimental data also support the hypothesis of the mitochondrial membrane depolarization after ROS generation at an early interval of apoptosis. We also observed ROS accumulation at different timepoints (early hours), but the results at the 24 h interval gave the maximum level of ROS generation in Con-treated cells.

In conclusion, the overall results suggest that Con has the anti-proliferative and anti-cancer potential. It works via induction of apoptosis by primarily targeting nuclear DNA and causing nuclear DNA damage, bringing the change in mitochondrial membrane potential and changing the capase-3 expression levels in the two NSCLC cell lines, thus indicating its ability to kill lung cancer cells as well, although it had been used mainly against stomach cancer by practitioners of traditional medicine including homeopathy. Further studies on *in vivo* animal models with this drug can prove to be rewarding.

ACKNOWLEDGEMENTS

This work was financially supported by a grant sanctioned to Prof. A.R. Khuda-Bukhsh, Dept. of Zoology, University of Kalyani by Boiron Laboratory, lyon, France. The authors are grateful to Boiron Laboratories, Lyon, France for financial support for the work.

CONFLICT OF INTEREST

All authors declare that there is no conflict of interest.

REFERENCES

Banerji P, Campbell DR, Banerji P. Cancer patients treated with the Banerji protocols utilising homoeopathic medicine: A best case series program of the National Cancer Institute USA. Oncol Rep. 2008; 20:69-74.

Biswas R, Mandal SK, Dutta S, Bhattacharyya SS, Boujedaini N, Khuda-Bukhsh AR. Thujone-rich fraction of Thuja occidentalis demonstrates major anti-cancer potentials: evidences from in vitro studies on A375 cells. Evid Based Complement Alternat Med. 2011;2011:568148.

Bolduc S, Denizeau F, Jumarie C. Cadmium-induced mitochondrial membrane-potential dissipation does not necessarily require cytosolic oxidative stress: studies using rhodamine-123 fluorescence unquenching. Toxicol Sci. 2004; 77:299-306.

Chakraborty D, Samadder A, Dutta S, Khuda-Bukhsh AR. Antihyperglycemic potentials of a threatened plant, Helonias dioica: antioxidative stress responses and the signaling cascade. Exp Biol Med. 2012;237:64-76.

Chen Y, McMillan-Ward E, Kong J, Israels SJ, Gibson SB. Mitochondrial electron-transport-chain inhibitors of complexes I and II induce autophagic cell death mediated by reactive oxygen species. J Cell Sci. 2007;120:4155-4166.

Denning MF, Wang Y, Tibudan S, Alkan S, Nickoloff BJ, Qin JZ. Caspase activation and disruption of mitochondrial membrane potential during UV radiation-induced apoptosis of human keratinocytes requires activation of protein kinase C. Cell Death Differ. 2002;9:40-52.

Guo W, Wu S, Liu J, Fang B. Identification of a small molecule with synthetic lethality for K-ras and protein kinase C iota. Cancer Res. 2008;68:7403-7408.

Jemal A, Murray T, Ward E, Samuels A, Tiwari RC, Ghafoor A, Feuer EJ, Thun MJ. Cancer statistics. CA Cancer J Clin. 2005;55:10-30.

Jürgensmeier JM, Xie Z, Deveraux Q, Ellerby L, Bredesen D, Reed JC. Bax directly induces release of cytochrome c from isolated mitochondria. Proc Natl Acad Sci USA. 1998;95:4997-5002.

Kim YM, Talanian RV, Billiar TR. Nitric oxide inhibits apoptosis by preventing increases in caspase-3-like activity via two distinct mechanisms. J Biol Chem. 1997; 272:31138-31148.

Kometani T, Yoshino I, Miura N, Okazaki H, Ohba T, Takenaka T, Shoji F, Yano T, Maehara Y. Benzo[a]pyrene promotes proliferation of human lung cancer cells by accelerating the epidermal growth factor receptor signaling pathway. Cancer Lett. 2009;278:27-33.

Kroemer G, Reed JC. Mitochondrial control of cell death. Nat Med. 2000;6:513-519.

Li P, Nijhawan D, Budihardjo I, Srinivasula SM, Ahmad M, Alnemri ES, Wang X. Cytochrome c and dATP-dependent formation of Apaf-1/caspase-9 complex initiates an apoptotic protease cascade. Cell. 1997;91:479-489.

Ling YH, Liebes L, Zou Y, Perez-Soler R. Reactive oxygen species generation and mitochondrial dysfunction in the apoptotic response to bortezomib, a novel proteasome inhibitor, in human H460 non-small cell lung cancer cells. J Biol Chem. 2003;278:33714-33723.

Misra R, Acharya S, Sahoo SK. Cancer nanotechnology: application of nanotechnology in cancer therapy. Drug Discov Today. 2010;15:842-850.

Morley N, Rapp A, Dittmar H, Salter L, Gould D, Greulich KO, Curnow A. UVA-induced apoptosis studied by the new apo/necro- comet assay which distinguishes viable, apoptotic and necrotic cells. Mutagenesis. 2006;21:105-114.

Mosmann T. Rapid colorimetric assay for cellular growth and survival: application to proliferation and cytotoxicity assays. J Immunol Methods. 1983;65:55-63.

Rostock M, Naumann J, Guethlin C, Guenther L, Bartsch HH, Walach H. Classical homeopathy in the treatment of cancer patients--a prospective observational study of two independent cohorts. BMC Cancer. 2011;11:19.

Samali A, Gorman AM, Cotter TG. Apoptosis -- the story so far..... Experientia. 1996;52:933-941.

Staunton MJ, Gaffney EF. Apoptosis: basic concepts and potential significance in human cancer. Arc Pathol Lab Med.

1998;122:310-319.

Su CC, Lin JG, Li TM, Chung JG, Yang JS, Ip SW, Lin WC, Chen GW. Curcumin-induced apoptosis of human colon cancer colo 205 cells through the production of ROS, Ca2+ and the activation of caspase-3. Anticancer Res. 2006;26:4379-4389.

Susin SA, Zamzami N, Kroemer G. Mitochondria as regulators of apoptosis: doubt no more. Biochim Biophys Acta. 1998; 1366:151-165.

Tan S, Sagara Y, Liu Y, Maher P, Schubert D. The regulation of reactive oxygen species production during programmed cell death. J Cell Biol. 1998;141:1423-1432.

Umehara K, Endoh M, Miyase T, Kuroyanagi M, Ueno A. Studies on differentiation inducers. IV. Pregnane derivatives from condurango cortex. Chem Pharm Bull. 1994;42:611-616.

Wang R, Song D, Jing Y. Traditional medicines used in differentiation therapy of myeloid leukemia. Asian J Trad Med. 2004;1-10.

Whitehead CM, Earle KA, Fetter J, Xu S, Hartman T, Chan DC, Zhao TL, Piazza G, Klein-Szanto AJ, Pamukcu R, Alila H, Bunn PA Jr, Thompson WJ. Exisulind-induced apoptosis in a non-small cell lung cancer orthotopic lung tumor model augments docetaxel treatment and contributes to increased survival. Mol Can Ther. 2003;2:479-488.

White A. Life, death, and the pursuit of apoptosis. Genes Dev. 1996;10:1-15.

Yang SC, Jenq SN, Kang ZC, Lee H. Identification of benzo[a]pyrene 7, 8-diol 9,10-epoxide N2-deoxyguanosine in human lung adenocarcinoma cells exposed to cooking oil fumes from frying fish under domestic conditions. Chem Res Toxicol. 2000;13:1046-1050.

Yeh CT, Yen GC. Effect of sulforaphane on metallothionein expression and induction of apoptosis in humanhepatoma HepG2 cells. Carcinogenesis 2005;26:2138-2140.